Journal of Applied Fluid Mechanics, Vol. 9, No. 3, pp. 1123-1134, 2016.
Available online at www.jafmonline.net, ISSN 1735-3572, EISSN 1735-3645.
DOI: 10.18869/acadpub.jafm.68.228.24475

Entropy Generation Analysis for Variable Thermal Conductivity MHD Radiative Nanofluid Flow through Channel

Md. S. Alam [1†], M. A. Alim[2] and M. A. H. Khan[2]

[1]*Department of Mathematics, Jagannath University, Dhaka-1100, Bangladesh*
[2]*Department of Mathematics, Bangladesh University of Engineering and Technology, Dhaka-1000, Bangladesh*

†*Corresponding Author Email: sarwar@math.jnu.ac.bd*

(Received January 9, 2015; accepted June 29, 2015)

ABSTRACT

The present work inspects the entropy generation on radiative heat transfer in the flow of variable thermal conductivity optically thin viscous Cu–water nanofluid with an external magnetic field through a parallel isothermal plate channel. Our approach uses the power series from the governing non-linear differential equations for small values of thermal conductivity variation parameter which are then analysed by various generalizations of Hermite- Padé approximation method. The influences of the pertinent flow parameters on velocity, temperature, thermal conductivity criticality conditions and entropy generation are discussed quantitatively both numerically and graphically. A stability analysis has been performed for the rate of heat transfer which signifies that the lower solution branch is stable and physically acceptable, whereas the upper solution branch is unstable.

Keywords: Channel flow; Thermal radiation; Variable thermal conductivity; Nanofluid; Irreversibility analysis; Bifurcation.

NOMENCLATURE

B_0	magnetic induction
b	dimensional length of the channel
Br	Brinkman number
C_p	specific heat of fluid at constant pressure
g	gravitational acceleration
Gr	Grashof number
H	Hartmann number
N	dimensionless pressure gradient
Nu	local Nusselt number
p'	dimensional pressure
P	dimensionless pressure
R	Radiation parameter
T_0	ambient temperature
$\overline{T}$	dimensional temperature
T_a	temperature of upper heated plate
u	dimensionless velocity
v'	velocity component along the y' axes
α	thermal conductivity variation parameter
β	thermal expansion coefficient
ϕ	nanoparticle volume fraction
η	dimensionless channel width
κ	thermal conductivity of the fluid
μ	dynamic viscosity of the fluid
ν	kinematic viscosity of the fluid
θ	dimensionless temperature
ρ	density of the fluid
σ	electrical conductivity

1. INTRODUCTION

Enhancing the heat transfer performance is essential in many industrial and engineering applications, such as heat exchangers, chemical processing equipment, electronic equipment cooling and so on. Heat transfer acts a significant role in many fields where the heating and cooling processes involved. Any substance with a temperature above absolute zero transfers heat in the form of radiation. Thermal radiation always exits and can strongly interact with convection in many situations of engineering interest. However, radiative heat transfer has a key impact in high temperature regime. Many technological processes occur at high temperature and good working knowledge of radiative heat transfer plays an instrumental role in designing the relevant equipment. In Cogley *et al.* (1968), the

differential approximation for radiative heat transfer in a nonlinear equation for gray gas near equilibrium was proposed. The thermal conductivity of the fluid had been assumed to be constant in many studies. However, it is known that this physical property may change significantly with temperature. For a liquid, it has been found that the thermal conductivity κ varies with temperature in an approximately linear manner in the range from 0 to 400^0F, as Kay (1966). Yasir *et al* (2011) analyzed the effects of variable viscosity and thermal conductivity on the flow and heat transfer in a laminar liquid film on a horizontal stretching sheet. Pinarbasi *et al*. (2011) investigates the effect of variable viscosity and thermal conductivity of a non-isothermal, incompressible Newtonian fluid flowing under the effect of a constant pressure gradient at constant temperatures in plane Poiseuille flow using Chebyshev pseudospectral method. Sadık *et al*. (2011) studied the effect of variable thermal conductivity and viscosity on single phase convective heat transfer in slip flow.

In the past few years, several simple flow problems associated with classical hydrodynamics have received new attention within the more general context of magnetohydrodynamics (MHD). A survey of MHD studies in the technological fields can be found in Moreau (1990). The small disturbance stability of MHD plane-Poiseuille flow was investigated by Makinde and Motsa (2001). Makinde (2003) analyzed magnetohydrodynamic stability of Plane Poiseuille flow using multideck asymptotic technique. It is observed in his analysis that the magnetic field has a stabilizing effect on the flow and that this stability increases with an increase in Hartmann number. Patra et al. (2014) examined radiation effect on MHD fully developed mixed convection in a vertical channel with asymmetric heating where they observed that an increase in radiation parameter leads to a decrease in the fluid temperature in the channel.

Kwak and Kim (2005) showed that heat transfer efficiency can be improved by increasing the thermal conductivity of the working fluid. Due to heat transfer mostly used fluids such as water, ethylene glycol, and engine oil have relatively low thermal conductivities compared to the thermal conductivity of solids. High thermal conductivity of solids can be used to increase the thermal conductivity of a fluid by adding small solid particles to that fluid. The feasibility of the usage of such suspensions of solid particles with sizes on the order of millimeters or micrometers was investigated by various researchers and significant advantages were observed in Khanafer *et al*. (2003). Recent advances in nanotechnology have allowed authors to study the next generation heat transfer nanofluids, a term first introduced by Choi (1995). Nanofluids are engineered dilute colloidal dispersions of nano-sized (less than 100 nm) particles in a base fluid as Das et al. (2007). Nanoparticles have unique chemical and physical properties in Oztop and Abu-Nada (2008) and have better thermal conductivity and radiative heat transfer compared to the base fluid only.

For any thermal system, as the entropy generation increases, the energy decreases. Thus, to enhance the efficiency of the system, the rate of entropy generation must be effectively controlled. The idea of thermodynamic irreversibility is central to the understanding of entropy. Everyone has an intuitive knowledge of irreversibility. The second law of thermodynamics states that all real processes are irreversible. Entropy generation provides a measure of the amount of irreversibility associated with real process. Bejan (1996) studied the entropy-generation for forced convective heat transfer due to temperature gradient and viscosity effects in a fluid. Bejan (1979) also presented various reasons for entropy-generation in applied thermal engineering where the generation of entropy destroys the available work of a system. The effect of thermal radiation and variable viscosity on entropy generation rate in the flow of optically thin fluid through channel was analysed by Makinde (2009) using Hermite–Padé approximation method. Mah et al. (2012) studied the entropy generation characteristics in a fully-developed forced convection flow of Al_2O_3–water nanofluid in a circular micro-channel. The results showed that when viscous dissipation effects are taken into account, the addition of nanoparticles increases the entropy generation rate and reduces the heat transfer effect since the greater thermal conductivity and viscosity of the nanofluid enhances both the heat transfer irreversibility and the fluid friction irreversibility. Chen et al. (2014) studied heat transfer and entropy generation in fully-developed mixed convection nanofluid flow in vertical channel. They analysed the effects of viscous dissipation on the entropy generation within vertical asymmetrically heated channels containing mixed convection flow.

However, the thermal boundary layer equation for variable thermal conductivity fluids in the presence of thermal radiation construct a nonlinear problem and the solution behavior will present an imminent into complex physical process of thermal instability in the system. Moreover, the models on classical semi-analytical methods have experienced a revival, in connection with the scheme of new hybrid numerical-analytical techniques for nonlinear differential equations, such as Hermite–Padé approximation method.

Taking into account the significance of variable thermal conductivity and thermal radiation effect on entropy generation rate in the flow of MHD conducting viscous nanofluid through a channel with non-uniform wall temperature is studied applying Hermite- Padé approximation. A stability analysis is also performed to show the physically realizable in practice of local Nusselt number due to thermal conductivity criticality. Results of the velocity, temperature, volumetric entropy generation rate and Bejan number for various values of the involved parameters are presented graphically.

2. MATHEMATICAL FORMULATION

Consider the steady, incompressible and laminar variable thermal conductivity flow of Cupper – water nanofluid in a parallel-plate channel. A two-dimensional Cartesian coordinate system is used and the flow is chosen along the x-direction under constant pressure gradient.

The top and bottom wall temperatures are non-uniform under radiative heat transfer and an externally homogeneous magnetic field is applied vertically to the top wall. The equations of continuity, momentum and energy considering viscous dissipation and buoyancy force for the problem are

$$\frac{\partial u'}{\partial x'}+\frac{\partial v'}{\partial y'}=0 \tag{1}$$

$$u'\frac{\partial u'}{\partial x'}+v'\frac{\partial u'}{\partial y'}=-\frac{1}{\rho_{nf}}\frac{\partial p'}{\partial x'}+\nu_{nf}\left(\frac{\partial^2 u'}{\partial x'^2}+\frac{\partial^2 u'}{\partial y'^2}\right) -\frac{\sigma_{nf}B_0{}^2}{\rho_{nf}}u'+g\beta(\overline{T}-T_0) \tag{2}$$

$$u'\frac{\partial v'}{\partial x'}+v'\frac{\partial v'}{\partial y'}=-\frac{1}{\rho_{nf}}\frac{\partial p'}{\partial y'}+\nu_{nf}\left(\frac{\partial^2 v'}{\partial x'^2}+\frac{\partial^2 v'}{\partial y'^2}\right) \tag{3}$$

$$\left(\rho c_p\right)_{nf}\left(u'\frac{\partial \overline{T}}{\partial x'}+v'\frac{\partial \overline{T}}{\partial y'}\right)=\kappa_{nf}\left(\frac{\partial^2 \overline{T}}{\partial x'^2}+\frac{\partial^2 \overline{T}}{\partial y'^2}\right) +\mu_{nf}\left(\frac{\partial u'}{\partial y'}\right)^2-\frac{\partial q}{\partial y'} \tag{4}$$

Since the velocity is only along x-direction and $v'=0$.

Eq. (1) reduces to $\frac{\partial u'}{\partial x'}=0$ which implies that u' depends on y only.

For simplicity $\frac{\partial \overline{T}}{\partial x'}=0,\quad \frac{\partial^2 \overline{T}}{\partial x'^2}=0$. Equations (2) and (4) takes the form

$$\frac{d^2u'}{dy'^2}-\frac{1}{\mu_{nf}}\frac{dp'}{dx'}-\frac{\sigma_{nf}B_0{}^2}{\mu_{nf}}u'+\frac{g\beta(\overline{T}-T_0)}{\nu_{nf}}=0 \tag{5}$$

$$\frac{1}{\left(\rho c_p\right)_{nf}}\left[\kappa_{nf}\frac{d^2\overline{T}}{dy'^2}-\frac{dq}{dy'}+\mu_{nf}\left(\frac{du'}{dy'}\right)^2\right]=0 \tag{6}$$

The boundary conditions are:

$$\begin{aligned} &y'=-b:\ u'=0,\ \overline{T}=T_0\\ &y'=b:\ u'=0,\ \overline{T}=T_a \end{aligned} \tag{7}$$

The corresponding dynamic viscosity, effective density, effective thermal conductivity and heat capacity of the nanofluid by Sreenivasulu and Reddy (2015) are

$$\mu_{nf}=\frac{\mu_f}{(1-\phi)^{2.5}},\quad \rho_{nf}=(1-\phi)\rho_f+\phi\rho_s,$$

$$k_{nf}=k_f\frac{k_s+2k_f-2\phi(k_f-k_s)}{k_s+2k_f+\phi(k_f-k_s)}$$

$$\left(\rho c_p\right)_{nf}=(1-\phi)\left(\rho c_p\right)_f+\phi\left(\rho c_p\right)_s$$

where ϕ is the solid volume fraction of nanoparticle.

The effective electrical conductivity of nanofluid was presented by Sheikholeslami (2012) as:

$$\frac{\sigma_{nf}}{\sigma_f}=1+\left[3\left(\frac{\sigma_s}{\sigma_f}-1\right)\phi/\left(\left(\frac{\sigma_s}{\sigma_f}+2\right)-\left(\frac{\sigma_s}{\sigma_f}-1\right)\phi\right)\right]$$

The radiative heat flux according to Cogley *et al.* (1968) is given by

$$\frac{dq}{dy'}=4\gamma^2(\overline{T}-T_0)$$

where γ is the mean radiation absorption coefficient.

Following Kay (1966), the variable thermal conductivity

$$\kappa_{nf}=\kappa_\infty\left[1+\varepsilon\left(\overline{T}-T_0\right)\right]$$

Where k_∞ is the thermal conductivity at the ambient temperature T_0 and ε is defined by $\varepsilon=\frac{1}{\kappa_{nf}}\left(\frac{\partial\kappa}{\partial\overline{T}}\right)_{nf}$.

The following transformations are considered

$$x=\frac{x'}{b},\ y=\frac{y'}{b},\ u=\frac{u'}{U},\quad p=\frac{b\,p'}{U},\ \theta=\frac{\overline{T}-T_0}{T_a-T_0},$$

$$H'^2=\frac{\sigma_f B_0{}^2b^2}{\mu_f},\quad Gr'=\frac{g\beta(T_a-T_0)b^2}{\nu_f U},$$

$$R'=\frac{4\gamma^2b^2}{\kappa_\infty},\ Br'=\frac{\mu_f U^2}{\kappa_\infty(T_a-T_0)},\quad N=-\frac{1}{\mu_f}\frac{dp}{dx},$$

$$\kappa=\frac{\kappa_{nf}}{\kappa_\infty},\quad \alpha=\varepsilon\left(T_a-T_0\right)$$

where U is the mean velocity.

The non-dimensional form of the Eqs (5)-(6) are

$$\frac{d^2u}{dy^2}-C(AH'^2u-BGr'\theta-N)=0 \tag{8}$$

$$[1+\alpha\theta]\frac{d^2\theta}{dy^2}-R'\theta+\frac{Br'}{C}\left(\frac{du}{dy}\right)^2=0 \tag{9}$$

Where,

$$A=1+\left[3\left(\frac{\sigma_s}{\sigma_f}-1\right)\phi/\left(\left(\frac{\sigma_s}{\sigma_f}+2\right)-\left(\frac{\sigma_s}{\sigma_f}-1\right)\phi\right)\right],$$

$$B = 1-\phi+\phi\frac{\rho_s}{\rho_f},\ C = (1-\phi)^{2.5}$$

The boundary conditions in dimensionless form

$$y=-1:\ u=0,\ \theta=0$$
$$y=1:\quad u=0,\ \theta=1$$

For simplicity of calculation we rescale by considering,

$$Gr=\frac{Gr'}{\alpha},\ H^2=\frac{H'^2}{\alpha},\ R=\frac{R'}{\alpha},\ Br=\frac{Br'}{\alpha}.$$

$$\frac{d^2u}{dy^2}-C(AH^2\alpha u-BGr\alpha\theta-N)=0 \qquad (10)$$

$$\frac{d^2\theta}{dy^2}+\alpha\theta\frac{d^2\theta}{dy^2}-R\alpha\theta+\frac{Br}{C}\alpha\left(\frac{du}{dy}\right)^2=0 \qquad (11)$$

Eqs (10)-(11) will be solved using both power series and Hermite- Padé approximation method.

3. SERIES ANALYSIS

The following power series expansions are considered in terms of the parameter α as equation (11) is non-linear for temperature field

$$\theta=\sum_{i=0}^{\infty}\theta_i\alpha^i,\quad u=\sum_{i=0}^{\infty}u_i\alpha^i,\quad |\alpha|<1 \qquad (12)$$

The non-dimensional governing equations (10) and (11) are then solved into series solutions by substituting the Eq. (12) and equating the coefficients of powers of α. With the help of algebraic programming language MAPLE, we have computed the first 18 coefficients for the series of the temperature $\theta(y)$ and velocity $u(y)$ in terms of $\alpha, H, R, Gr, Br, N, A, B, C$ respectively. The first few coefficients of the series for $\theta(y)$ and $u(y)$ are as follows:

$$\begin{aligned}\theta(y;\alpha,R,H,Br,Gr,N)&=\frac{1}{2}+\frac{1}{2}y-\frac{1}{12}(y-1)(y+1)\\&(BrCN^2y^2-Ry-3R+BrCN^2)\alpha-\frac{1}{720}(y-1)\\&(y+1)(2Ry^4BrCN^2+8BrC^2N^2y^4AH^2\\&-18BrCN^2y^3-3y^3R^2+18BrCNy^3BGr\\&-30BrCN^2y^2-15y^2R^2+60BrCNy^2BGr\\&+15y^2R-52BrC^2N^2y^2AH^2+2BrCN^2y^2R\\&-18BrCN^2y+60Ry+7R^2y-2BrCNyBGr\\&-28BrCN^2R-30BrCN^2+105R+75R^2\\&+60BrCNBGr-52BrC^2N^2AH^2)\alpha^2\\&+O(\alpha^3)\end{aligned} \qquad (13)$$

The obtained power series solutions are valid for very small values of α. Therefore, the series are analysed applying Hermite- Padé approximation method, as demonstrated in the following section.

$$\begin{aligned}u(y;\alpha,R,H,Br,Gr,N)&=-\frac{1}{2}NC(y-1)(y+1)\\&-\frac{1}{24}C(y-1)(y+1)(AH^2CNy^2-5AH^2CN+2BGry\\&+6BGr)\alpha-\frac{1}{720}C(y-1)(y+1)(A^2H^4C^2Ny^4\\&-2BGry^4BrCN^2+3AH^2Cy^3BGr+3BGry^3R-\\&14A^2H^4C^2Ny^2+15AH^2Cy^2BGr+15BGrRy^2\\&-2Cy^2BGrBrN^2-7AH^2CBGry-7BGrRy\\&+28BGrBrCN^2+61A^2H^4C^2N-75AH^4CBGr\\&-75BGrR)\alpha^2+O(\alpha^3)\end{aligned} \qquad (14)$$

4. HERMITE-PADÉ APPROXIMANTS

The idea of thermal conductivity criticality or non-existence of steady-state solution to nonlinear thermal boundary layer equations for certain parameter values, is extremely important from physical point of view. This typifies the thermal stability conditions of the materials under consideration and the onset of thermal runaway characteristics. To compute the criticality conditions in the system, we shall employ a very efficient solution method, known as Hermite-Padé approximants, which was first introduced by Padé (1892) and Hermite (1893).

We say that a function is an *approximant* for the series

$$S=\sum_{n=0}^{\infty}s_n\alpha^n \qquad (15)$$

if it shares with S the same first few series coefficients at $|\alpha|<1$. Thus, the simplest approximants are the partial sums of the series S. When the series converges rapidly, such *polynomial* approximants can provide good approximations of the sum.

In the Padé method, the approximant is sought in the class of *rational* functions. When applied to the Nth partial sum of the series (15), it involves the construction of two polynomials in α, say $P_N^{(0)}$ and $P_N^{(1)}$, such that $\deg P_N^{(0)}+\deg P_N^{(1)}+1=N$ and

$$P_N^{(0)}S+P_N^{(1)}=O(\alpha^N)\ \text{ as }\ |\alpha|<1 \qquad (16)$$

The rational approximant S_N is then defined by

$$P_N^{(0)}S_N+P_N^{(1)}=0 \qquad (17)$$

We emphasize that only the first N coefficients s_n of the series S are required in order to construct the $P_N^{(l)}$. The second equation in (16) can be expressed as a linear system of equations for the unknown

coefficients of the polynomials $P_N^{(l)}$. In order to obtain a unique solution, one must normalize in some way; for example by setting

$$P_N^{(0)}(0) = 1$$

The first equation in (16) then simply ensures that the matrix associated with the system is square. The poles of S_N are the zeros of the polynomial $P_N^{(0)}$ and the hope is that one of these zeros, say $\alpha_{c,N}$, tends to the location, say α_c, of the dominant singularity of *S* as *N* increases. In practice, one finds that the method is most accurate when the dominant singularity of *S* is a pole.

The principle underlying any approximant method is that the problem to which it is applied is replaced by a more tractable problem involving polynomial coefficients. Given a particular problem, the ideal approximant method replaces it by one that is rich enough to reproduce the essential features of the true solution, but simple enough that these features can be deduced easily once the polynomial coefficients are known.

Hermite-Padé approximants generalizes the Padé method in the following sense: Given *d* power series $S^{(1)},.....,S^{(d)}$, one construct polynomials $P_N^{(l)}$ such that

$$\deg P_N^{(0)} + \deg P_N^{(1)} + ... + \deg P_N^{(d)} + d = N \tag{18}$$

And

$$P_N^{(0)} S^{(d)} + P_N^{(1)} S^{(d-1)} + ... + P_N^{(d)} = O(\alpha^N) \quad \text{as } |\alpha| < 1 \tag{19}$$

For functions with logarithmic or algebraic singularities, special types of Hermite-Padé approximants can sometimes outperform the Padé method. For instance, suppose that

$$S(\alpha) - S_0 \sim S_1(\alpha_c - \alpha)^{\delta} \quad \text{as } \alpha \to \alpha_c \tag{20}$$

Then a good summation method is to choose a suitably large natural number *d*, set

$$S^{(l)} = S^l, \quad 1 \le l \le d, .$$

and define an *algebraic* approximant S_N of *S* by

$$P_N^{(0)} S_N^d + P_N^{(1)} S_N^{d-1} + ... + P_N^{(d)} = 0. \tag{21}$$

Note that, for $d > 1$, S_N is a multivalued function of α with *d* branches. Furthermore, its singularities are of the form

$$S_N(\alpha) - S_{0,N} \sim S_{1,N}(\alpha_{c,N} - \alpha)^{\delta_N} \quad \text{as } \alpha \to \alpha_{c,N}, \tag{22}$$

where the numbers $S_{0,N}, S_{1,N}, \delta_N$ and $\alpha_{c,N}$ can be deduced easily from the polynomials $P_N^{(l)}$. Thus, if the assumption (20) is valid, then these numbers can provide good approximations of the true singularity parameters S_0, S_1, δ and α_c for *N* sufficiently large.

Alternatively, one may use

$$S^{(l)} = D^{l-1} S, \quad 1 \le l \le d,$$

where *D* denotes differentiation with respect to α, and define a *differential* approximant S_N of *S* by

$$P_N^{(0)} D^{d-1} S_N + P_N^{(1)} D^{d-2} S_N + ... + P_N^{(d)} = 0. \tag{23}$$

In order to characterize the approximant S_N completely, one must choose the degree of each of the polynomials $P_N^{(l)}$ in (18). A popular strategy is to take

$$\deg P_N^{(0)} = ... = \deg P_N^{(d)}, \quad d \text{ fixed and } N \to \infty. \tag{24}$$

In the case of algebraic approximants, we take $P_N^{(l)}$ so that

$$P_N^{(0)} S^d + P_N^{(1)} S^{d-1} + ... + P_N^{(d)} = [S(\alpha) - S(0)]^N$$

for $N = 0, 1, ..., d$.

In the case differential approximants, we set, for $N = 0, 1, ..., d$.

$$P_N^{(l)} = \begin{cases} 0 & \text{if } l < d - N, \\ 1 & \text{if } l = d - N, \end{cases}$$

and let $P_N^{(l)}$ for $l > d - N$ be constants such that (19) holds. Such constants can be calculated by solving a simple linear system of equations.

Drazin and Tourigny (1996) proposed a different strategy for constructing algebraic approximants in which one takes

$$\deg P_N^{(l)} = l \quad \text{for} \quad 0 \le l \le d \quad \text{and} \quad N = \frac{d}{2}(d+3) \text{ as } d \to \infty. \tag{25}$$

Generically, the singularities $\alpha_{c,N}$ of S_N correspond to zeroes of the leading coefficient. Hence

$$P_N^{(0)}(\alpha_{c,N}) = 0.$$

If the singularity is of algebraic type, then the exponent δ may be approximated by

$$\delta_N = d - 2 - \frac{P_N^{(1)}(\alpha_{c,N})}{D P_N^{(0)}(\alpha_{c,N})}. \tag{26}$$

Khan (2002) introduced High-order differential approximant (HODA) as a special type of

differential approximants.

5. ENTROPY GENERATION

Flow properties inside a channel with isothermal walls in the presence of thermal radiation and MHD effect are irreversible. The exchange of energy and momentum, within the fluid and at solid boundaries causes inequilibrium conditions which leads to continuous entropy generation. Following Bejan (1996) the volumetric entropy generation rate is given as

$$E_G = \frac{\kappa_\infty}{T_0^{\,2}}\left(\frac{d\bar{T}}{dy'}\right)^2 + \frac{\mu_{nf}}{T_0}\left(\frac{du'}{dy'}\right)^2 \tag{27}$$

Where the first term on the right side of equation (27) is the irreversibility due to heat transfer and the second term is the irreversibility due to viscous dissipation. The entropy generation number can be expressed in dimensionless form as

$$N_S = \frac{T_0^{\,2} b^2 E_G}{\kappa_\infty (T_a - T_0)^2} = \left(\frac{d\theta}{dy}\right)^2 + \frac{Br}{\Omega(1-\phi)^{2.5}}\left(\frac{du}{dy}\right)^2 \tag{28}$$

Where $\Omega = \dfrac{(T_a - T_0)}{T_0}$ is the temperature difference parameter and

$$N_1 = \left(\frac{d\theta}{dy}\right)^2, \quad N_2 = \frac{Br}{\Omega(1-\phi)^{2.5}}\left(\frac{du}{dy}\right)^2$$

In general, the entropy generation number N_s given in Eq. (28) provides a useful means of producing entropy generation profiles. However, it gives no indication as to the relative contributions of the fluid heat transfer and fluid friction effects. Thus, the parameter, Bejan number *Be* is commonly used in its place.

The Bejan number is given as $Be = \dfrac{N_1}{N_S}$

It is noteworthy that the Bejan number ranges from 0 to 1 and $Be = 0$ is the limit where the irreversibility is dominated by fluid friction effects. $Be = 1$ is the limit where the irreversibility due to heat transfer dominates the flow system because of finite temperature differences. The contributions of heat transfer and fluid friction to entropy generation are equal when $Be = 1/2$.

6. RESULTS AND DISCUSSION

In this paper we focus on the combined effect of thermal radiation and temperature dependent variable thermal conductivity on the entropy generation of MHD nanofluid flow in channel. The minimum entropy conditions provide the possibility of achieving the maximum available work. The densities of the base fluid and Cu-nanoparticles are respectively 998.1 (kg/m^3), 8933(kg/m^3). It is essential to note here that Eq. (13) can be used to approximate the series for the wall heat flux parameter in terms of Nusselt number $Nu = -d\theta/dy$ at $y = 1$.

In the present study, the nanoparticle volume fraction is specified in the range of $\phi = 0\% - 10\%$, where a value of $\phi = 0$ indicates the pure base fluid. In addition, the thermal conductivity variation parameter is assigned in the range of $-0.1 \le \alpha \le 0.9$, the radiation parameter $0 \le R \le 10$, the Brinkman number $1 \le Br \le 50$, the Hartmann number $0 \le H \le 4$. The Grashof number and dimensionless pressure gradient kept fixed at $Gr = 1,\ N = 1$.

6.1 Stability Analysis

Table 1 represents that the critical values of thermal conductivity variation parameter α_c increase with a positive increase in the values of radiation parameter *R* and the values of δ_c indicates that α_c is a branch point. Therefore, it is significant to notice from the table that as the radiation effect enhances, the progress of thermal runaway reduces and the thermal stability in the system improves. While the negative values of radiation parameter may lessen the magnitude of the criticality parameter and accelerate thermal runaway in the system.

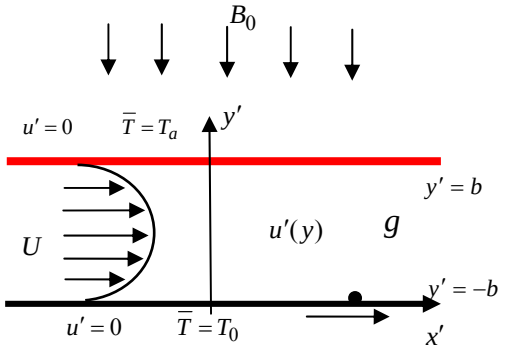

Fig. 1. Geometry of the problem.

However, in presence of nanofluid ($\phi = 5\%$), both the rate of heat transfer *Nu* and α_c enhances as *R* increases. This implies that the heat transfer performance is higher in nanofluid than base fluid. Finally the values of α_c in Table 1 give an idea about the onset of thermal instability and its nature numerically. A segment of bifurcation diagram for different values of *d* in the (α, Nu) plane is noticed in Fig. 2(a) using Drazin-Tourigny Approximants. It is interesting to notice that there are two solution branches (I and II) of Nusselt number when $\alpha > \alpha_c$, one solution when $\alpha = \alpha_c$, and no solution when $\alpha < \alpha_c$, where α_c is the critical value of α for which the solution exists. The stability analysis indicates that the lower solution branch (II) is stable and physically realizable. For different values of *d*, the upper solution branch (I) is unstable

Table 1 Numerical calculations showing thermal conductivity criticality for different parameter values using High-order Differential Approximants at $Br = 1, Gr = 1, H = 1, N = 1$.

R	ϕ	α_c	δ_c	Nu
0.5	0	-0.72295638183	0.489985004	-0.1897709072
1	0	-0.53565727924	0.464278610	0.1864302964
2	0	-0.37733219733	0.449667446	0.5561558067
5	0	-0.21641937233	0.456544910	1.130723424
2	0.05	-0.37328441444	0.449147585	0.6115499181
5	0.05	-0.21567016329	0.453808805	1.154478277

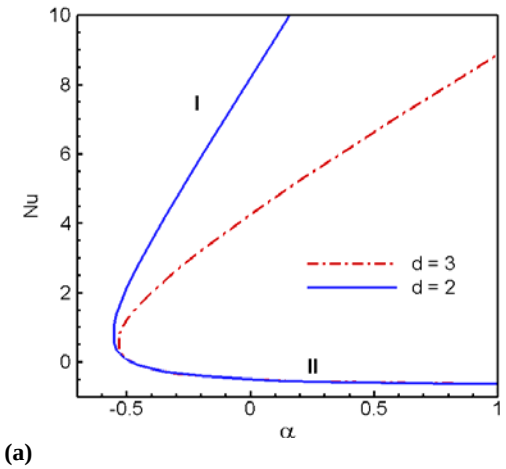

(a)

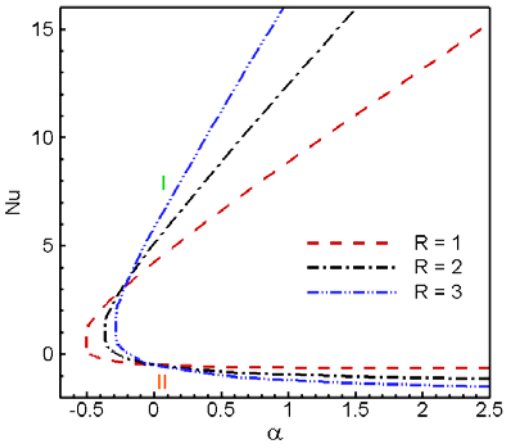

(b)

Fig. 2. Approximate bifurcation diagrams of α **in the** $(\alpha,\ Nu(1))$ **plane (a) for different *d* and (b) for different *R* obtained by Drazin-Tourigny method (1996) for** $N = 1, Gr = 1,$ $Br = 1, H = 1, R = 1, d = 3$.

and physically unacceptable as shown in Fig. 2(a). Figure 2(b) represents the effect of radiation parameter *R* on the bifurcation diagram in the way that the bifurcating point increases as *R* increases uniformly and produces more instability to the upper solution branch (I). The numerical values in Table 1 are also consistent with the lower solution branch of *Nu* as *R* increases for negative values of α in Fig. 2(b). Moreover, the local rate of heat transfer decreases very slowly in lower solution (II) as *R* increases due to radiative heat loss for positive increase of α .

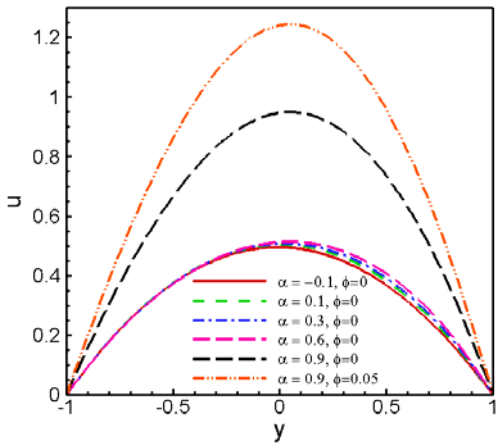

Fig. 3. Velocity profile for different values of α **at** $R = 1, N = 1, Gr = 1, Br = 1, H = 1$.

6.2 Effect of Thermal Conductivity Variation Parameter

Figures 3-6 represent the effects of thermal conductivity variation parameter on velocity profiles, temperature distribution, entropy generation rate N_s and distribution of Bejan number *Be* respectively. It is observed in Fig. 3 that increasing value of α results in slow increment in fluid velocity and for nanofluid there is a significant improvement in fluid motion approximately by 20% along the centerline region as α increases. As the thermal conductivity increases, the heat is more readily transferred particularly in nanofluid which leads to enhancement of fluid velocity within the centerline. A decrease in the fluid temperature around the central region of the channel is observed in Fig.4 due to the escalating values of α. The increases of thermal conductivity variation parameter produce more heat transfer within the channel centerline region and reduce dimensionless temperature distribution. Furthermore, due to the

higher thermal conductivity coefficient of the nanofluid, the heat is more keenly transferred.

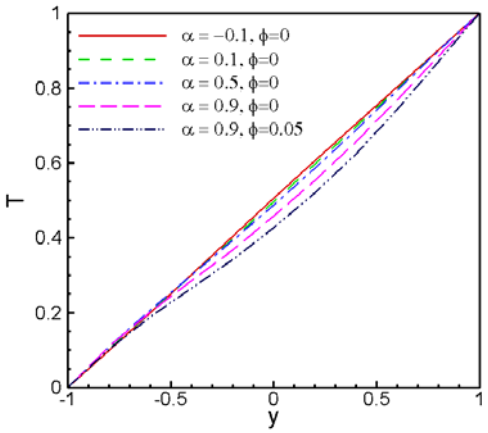

Fig.4. Temperature profile for different values of α at $H=1, N=1, Gr=1, Br=1, R=0.5$.

Generally, the value of N_2 i.e., the entropy generated by fluid friction is larger than that of N_1 i.e., the entropy produced by fluid heat transfer. As a result, N_S is contributed mainly by N_2 throughout the entire flow field. However, in the areas of the flow field characterized by a faster flow rate, the velocity gradient is reduced, and thus N_2 also reduces. In the present parallel channel, N_S gradually reduces to zero at $y = -0.5$ as shown in Fig.5. In this particular region of the flow field, fluid friction effects play only a minor role, and thus N_S is contributed mainly by N_1.

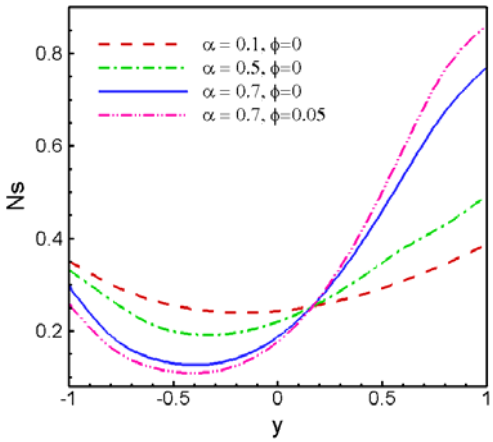

Fig. 5. Entropy generation rate for different values of α : $N=1, Gr=1, Br=1, H=1, R=1$.

Figure 5 illustrates the entropy generation rate when α is increasing and other parameters remain constant. The entropy production number N_S closely similar from lower wall to centerline and then to the upper wall for lesser values of α, but for rising values α, N_S increases rapidly in base fluid and further in nanofluid in the region above the centerline to the hot wall. However, in the region below the centerline to the cold wall N_S decreases as α increases, because the dominant effect of heat transfer occurs at the upper hot wall.

Figure 6 displays the distribution of the Bejan number (*Be*) versus the channel width for thermal conductivity variation parameter α. It is noticed that *Be* has a value of less than 1 on either side of the channel since, as discussed previously, the velocity gradient is increased at the cold and hot sides of the channel, and hence N_S is contributed initially by N_2. In the central region of the flow field, *Be* increases to a maximum value of 1 due to the reduction in the velocity gradient and the corresponding increase in the contribution of N_1 to the overall entropy generation. It is to be seen that heat transfer irreversibility dominates the flow process within the channel centerline region, while the little influence of fluid friction irreversibility can be observed at the walls. It is seen in Fig. 6 that from lower cold wall to centerline region *Be* decreases as α increases and conversely from centerline region to upper hot wall *Be* increases as α increases.

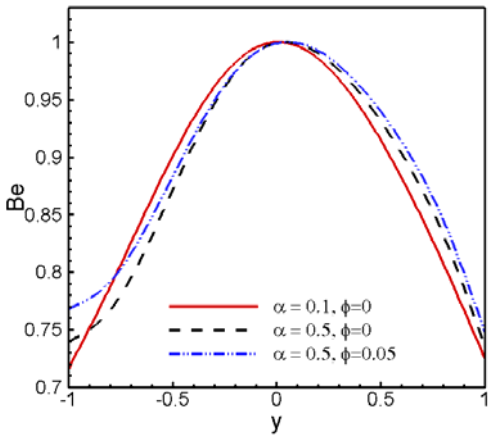

Fig. 6. Bejan number for different values of α : $N=1, Gr=1, Br=1, H=1, R=1$.

6.3 Effect of Radiation Parameter

The influences of radiation parameter on velocity profiles,

temperature distribution, entropy generation rate N_s and

distribution of Bejan number *Be* are depicted in Figs.7-10. Figure 7 shows that the velocity slowly decreases as *R* increases and a decrement of nearly 12% in the velocity at centerline is seen in nanofluid when *R* increases due to radiation heat loss. The temperature decrease is further strengthened with rising values of the radiation parameter *R* for base fluid and nanofluid shown in Fig. 8. As *R* increases, the rate of heat loss accelerates around the center of the channel that generates reduction of the temperature profiles. As nanofluid exhibits higher rate of heat transfer, the reduction of the temperature profile becomes faster

in nanofluid as shown in Fig. 8.

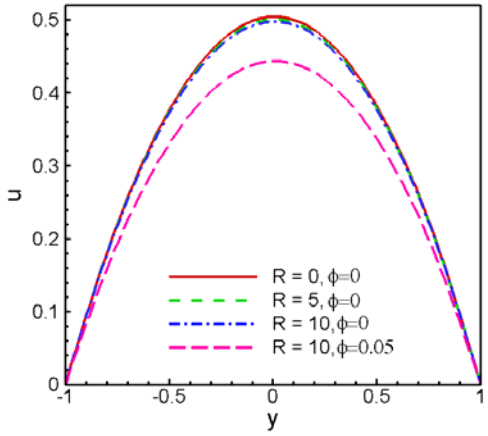

Fig. 7. Velocity profile for different values of *R* at $N=1, Gr=1, Br=1, H=1,\ \alpha=0.1$.

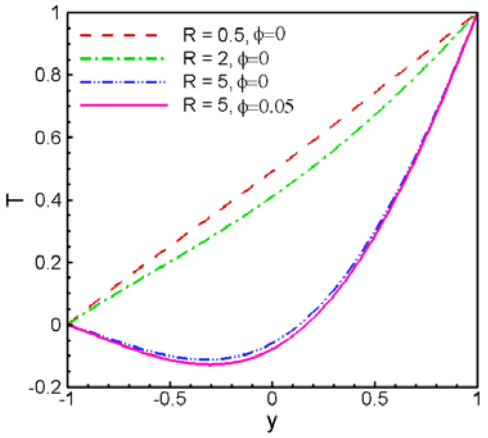

Fig. 8. Temperature profile for different values of *R* at $H=1, N=1, Gr=1, Br=1, \alpha=0.3$.

Figure 9 depicts the similar conjecture for N_S as α when R increases except the reduction of N_S in nanofluid around the upper hot wall due to the lesser viscous dissipation effect. It is to be noted from Fig.10 that heat transfer irreversibility dominates the flow process within the channel centerline region, while the little influence of fluid friction irreversibility can be observed at the walls. It is also seen in Fig. 10 that from lower cold wall to centerline region *Be* decreases as *R* increases and conversely from centerline region to upper hot wall *Be* increases as *R* increases.

6.4 Effect of Hartmann Number

Figures 11-13 represent the flow characteristics with entropy generation due to the effect of Hartmann number. In Fig 11 it is depicted that the velocity decreases for the positive changes of H and a reduction of around 40% in centerline velocity is found for the variation of $H=0$ to $H=4$. The variation of H leads to the variation of the Lorentz force due to magnetic field and the Lorentz force produces more resistance to the fluid velocity.

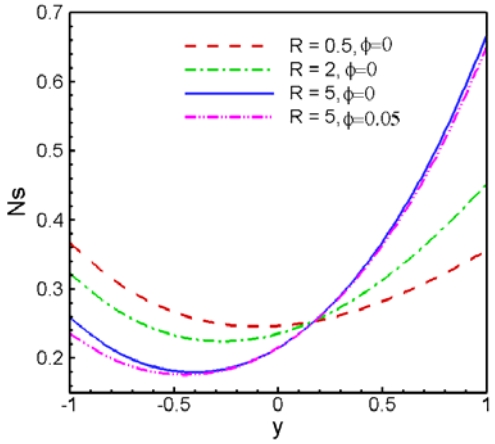

Fig. 9. Entropy generation rate for different values of *R* at $N=1, Gr=1, Br=1, H=1,\ \alpha=0.1$.

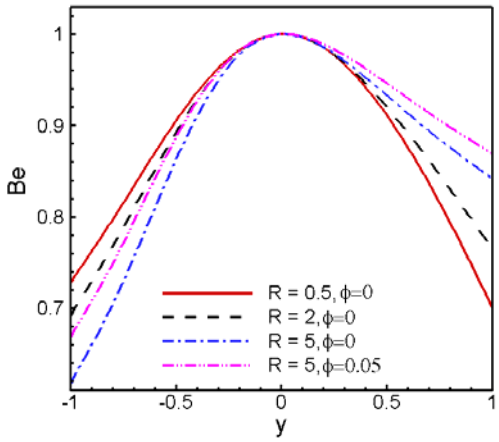

Fig. 10. Bejan number for different values of *R* at $N=1, Gr=1, Br=1, H=1,\ \alpha=0.1$.

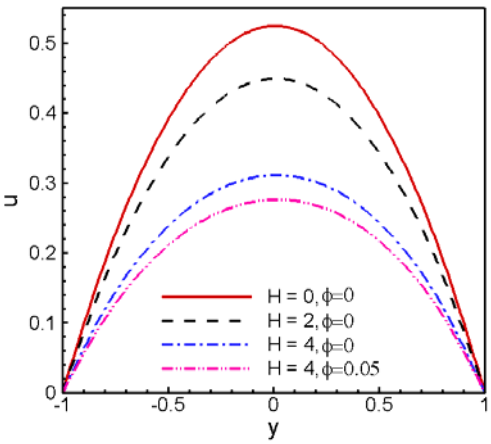

Fig. 11. Velocity profile for different values of *H* at $N=1, Gr=1, Br=1, R=1,\ \alpha=0.1$.

It is seen from Fig. 12 that Hartmann number H acts to reduce the entropy generation rate uniformly and N_S is lowest within the channel centerline increases towards both the walls particularly more at the upper wall. Figure 13 demonstrates that as Hartmann number H increases, the fluid friction irreversibility at the walls decreases significantly and further in nanofluid. The Lorentz force due to magnetic field produces more resistance to the fluid friction irreversibility and hence enhances the dominance effect of heat transfer irreversibility.

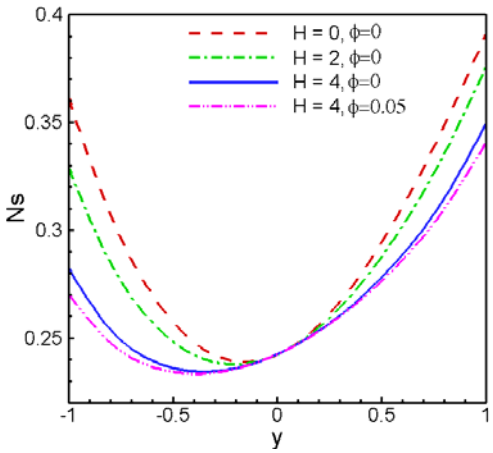

Fig. 12. Entropy generation rate for different values of H at $N=1, Gr=1, Br=1, R=1, \alpha=0.1$.

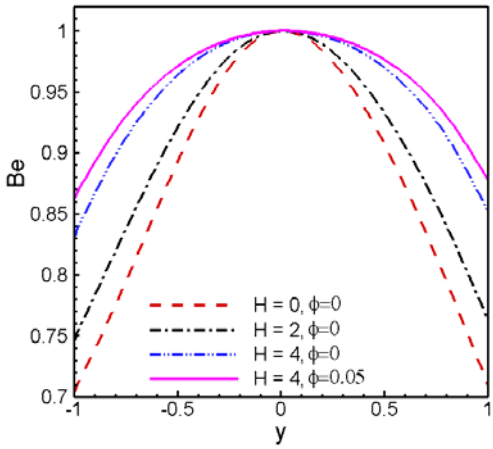

Fig. 13. Bejan number for different values of H at $N=1, Gr=1, Br=1, R=1, \alpha=0.1$.

6.5 Effect of Nanoparticles solid volume fraction

The control of nanoparticles volume fraction on flow field and entropy generation are presented in Figs. 14-16.

In Fig.14, a uniform reduction in fluid velocity is observed as ϕ increases. The equivalent thermal expansion coefficient of the nanofluid is less than that of base water. As a result, the buoyancy force acting on the nanofluid is also less than that acting on the pure water, and hence the dimensionless velocity is reduced. In addition, since the density and viscosity of the nanofluid are greater than those of base water, the velocity distribution within the channel is more uniform.

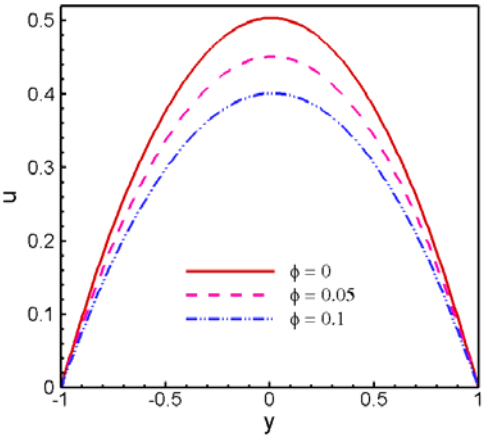

Fig. 14. Velocity profile for different values of ϕ at $N=1, Gr=1, Br=1, H=1, \alpha=0.1, R=1$.

Figure 15 shows the effect of an increase in volume fraction of nanoparticles on entropy generation rate. A uniform reduction is observed at the walls to N_S when ϕ increases. Therefore, nanofluid is suitable to reduce the entropy generation rate and to enhance the efficiency of the system. The mounting values of ϕ causes an identical increment of Be at the two walls symmetrically indicating governance effect of heat transfer irreversibility for nanofluid as shown in Fig.16.

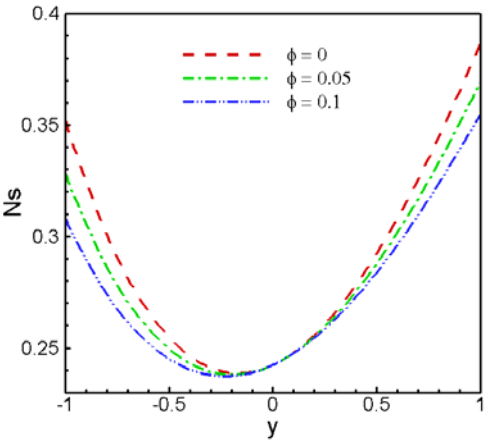

Fig.15. Entropy generation rate for different values of ϕ at $N=1, Gr=1, Br=1, H=1, \alpha=0.1, R=1$.

6.6 Effect of Brinkman Number

The dimensionless velocity distribution of the flow field has a direct effect on the dimensionless temperature distribution as the effects of viscous dissipation are taken into consideration in the present problem. It is noticed from Fig.17 that the fluid temperature increases with increasing

parametric values of viscous heating parameter *Br* but a minor reduction is seen in presence of nanoparticles. The velocity gradient of the pure working fluid is greater than that of the nanofluid due to the lower viscosity which results in more viscous dissipation effect. Furthermore, due to the higher thermal conductivity coefficient of the nanofluid, the heat is more intensely transferred. Hence, the dimensionless temperature of the nanofluid is less than that of the base fluid in Fig. 17.

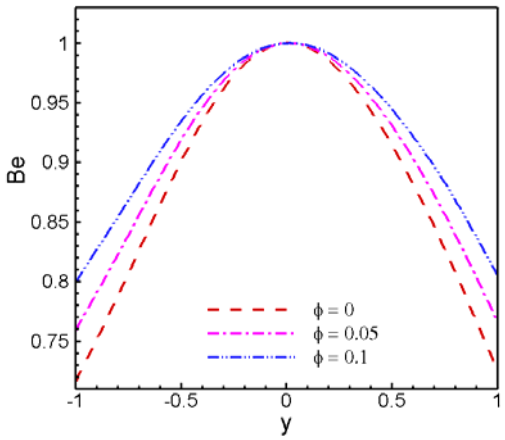

Fig. 16. Bejan profiles for different values of ϕ at $N=1, Gr=1, Br=1, H=1, \alpha=0.1, R=1$.

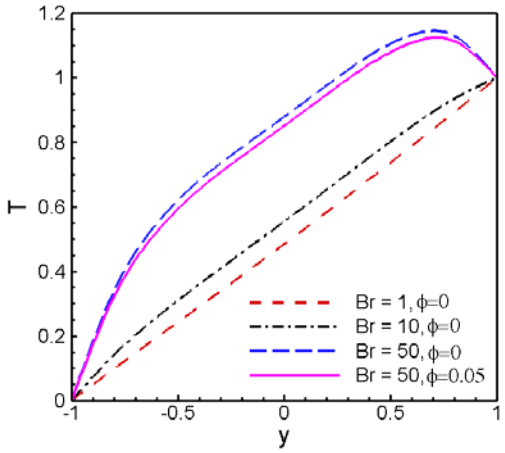

Fig. 17. Temperature profile for different values of *Br* at $H=1, N=1, Gr=1, R=1, \alpha=0.1$.

Thus thermal radiation and variable thermal conductivity play an imperative role to fluid friction and heat transfer irreversibility in modeling boundary layer flows with nanofluids through a channel. Physically the variation of thermal conductivity controls the rate of heat transfer. Moreover, the point of existence of two solution branches of which the lower one is physically acceptable, is determined by temperature dependent variable thermal conductivity. Finally, thermal radiation in presence of nanofluids has a key impact on the physical solution.

7. CONCLUSIONS

A numerical investigation is performed to the radiative heat transfer performance, temperature varied thermal conductivity effects and entropy generation characteristics of MHD Cu-water nanofluid flow through a channel with asymmetric heated wall applying Hermite-Padé approximants method. The dominating singularity behavior of the thermal conductivity variation parameter and the thermal stability conditions for two solution branches are analysed with the effect of Radiation parameter. An increase in the thermal conductivity variation parameter advances fluid velocity along centerline and reduces temperature distribution. Radiation parameter reduces both fluid velocity and temperature distribution due to faster heat loss. Increasing Hartmann number and nanoparticles solid volume fraction cause the reduction of fluid velocity near the centerline uniformly because of the acting of Lorentz force and reduction of buoyancy force respectively. For regions of the flow field at a greater velocity gradient, i.e., adjacent to the hot and cold walls, the total entropy generation rate is dominated by the effects of fluid friction. Conversely, in the regions of the flow field at a higher and more uniform velocity distribution, i.e., the central region of the channel, the total entropy generation rate is dominated by the effects of fluid heat transfer.

ACKNOWLEDGEMENTS

This work is done within the framework of the PhD program of the corresponding author under Department of Mathematics, Bangladesh University of Engineering and Technology, Dhaka. Financial support from the Bangabandhu Fellowship on Science and ICT project is acknowledged.

REFERENCES

Arpaci, V. S., A. Selamet and S. H. Kao (2000). *Introduction to Heat Transfer*. Prentice-Hall, New York.

Bejan, A. (1979). A study of entropy generation in fundamental convective heat transfer. *J. Heat Transfer* 101, 718-725.

Bejan, A. (1996). *Entropy-generation minimization*. CRC Press, New York.

Chang, L.C., K. T. Yang and J. R. Lloyd (1983). Radiation natural convection interaction in two-dimensional complex enclosure. *J. Heat Transfer* 105, 89–95.

Chawla, T. C. and S. H. Chan (1980). Combined radiation and convection in thermally developing Poiseuille flow with scattering. *J. Heat Transfer* 102, 297–302.

Chen, C. K., B. S. Chen and C. C. Liu (2014). Heat transfer and entropy generation in fully-developed mixed convection nanofluid flow in vertical channel. *Int. J. Heat Mass Transfer* 79, 750-758.

Choi, S. U. S. (1995). Enhancing thermal conductivity of fluids with nanoparticles. In *Proceedings of the 1995 ASME International Mechanical Engineering Congress and Exposition.* 66, San Francisco USA 99–105.

Cogley, A. C. L., W. G. Vincenti and E. S. Gilles (1968). Differential approximation for radiative heat transfer in a nonlinear equations-grey gas near equilibrium. *Am. Inst. Aeronaut. Astronaut. J.* 6, 551–553.

Das, S. K., S. U. S. Choi, W. Yu and T. Pradeep (2007). *nanofluids: Science and Technology*. Wiley, New York.

Drazin, P. G. and Y. Tourigny (1996). Numerically study of bifurcation by analytic continuation of a function defined by a power series. *SIAM Journal of Applied Mathematics* 56, 1-18.

Hermite, C. (1893). Sur la généralisation des fractions continues algébriques. *Annali di Mathematica Pura e Applicata* 21(2), 289-308.

Kay, W. M. (1966). *Convective heat and mass transfer*. Mc-Graw Hill, New York.

Khan, M. A. H. (2002). High-Order Differential Approximants. *Journal of Computational and Applied Mathematics* 149, 457-468.

Khanafer, K., K. Vafai and M. Lightstone (2003). Buoyancy-driven heat transfer enhancement in a two-dimensional enclosure utilizing nanofluids. *Int. J. Heat Mass Transfer* 46, 3639–3653.

Kwak, K. and C. Kim (2005). Viscosity and thermal conductivity of copper nanofluid dispersed in ethylene glycol. *Korea–Aust. Rheol. J.* 17, 35–40.

Mah, W. H., Y. M. Hung and N. Q. Guo (2012). Entropy generation of viscous dissipative nanofluid in microchannels. *Int. J. Heat Mass Transfer* 55(15-16), 4169-4182.

Makinde, O. D. (2003). Magneto-hydrodynamic stability of plane-Poiseuille flow using multi-deck asymptotic technique. *Math. Comput. Model.* 37(3-4), 251–259.

Makinde, O. D. (2008). Thermal criticality in viscous reactive flows through channels with a sliding wall: An exploitation of the Hermite-Padé approximation method. *Math. and Comp. Modelling* 47, 312-317.

Makinde, O. D. (2009). Hermite-Padé approach to thermal radiation effect on inherent irreversibility in a variable viscosity channel flow. *Comp. and Math. with Applications* 58, 2330-2338.

Makinde, O. D. and S. S. Motsa (2001). Hydromagnetic stability of plane Poiseuille flow using Chebyshev spectral collocation method. *J. Ins. Math. Comput. Sci.* 12(2), 175–183.

Moreau, R. (1990). *Magnetohydrodynamics*. Kluwer Academic Publishers, Dordrecht.

Oztop, H. F. and E. Abu-Nada (2008). Numerical study of natural convection in partially heated rectangular enclosures filled with nanofluids. *Int. J. Heat Fluid Flow* 29, 1326–1336.

Padé, H. (1892). Sur la représentation approchée d'une fonction pour des fractions rationnelles. *Ann. Sci. École Norm. Sup. Suppl.* 9, 1-93.

Patra, R., S. Das and R. N. Jana (2014). Radiation effect on MHD fully developed mixed convection in a vertical channel with asymmetric heating. *J. Applied Fluid Mechanics* 7(3), 503-512.

Pinarbasi, A., O. Coskun and D. Selim (2011). Influence of variable thermal conductivity and viscosity for nonisothermal fluid flow. *Physics of Fluids* 17(3), 038109-4.

Sadık, K., G. Almıla, Yazıcıoğlu and C. G. Arif (2011). Effect of variable thermal conductivity and viscosity on single phase convective heat transfer in slip flow. *Heat and Mass Transfer* 47(8), 879-891.

Sahin, A. Z. (1999). Effect of variable viscosity on the entropy generation and pumping power in a laminar fluid flow through a duct subjected to constant heat flux. *Heat Mass Transfer* 35, 499-506.

Sheikholeslami, M., S. Soleimani, M. Gorji-Bandpy, D. Ganji and S. Seyyedi (2012). Natural convection of nanofluids in an enclosure between a circular and a sinusoidal cylinder in the presence of magnetic field. *Int. Com. in Heat and Mass transfer* 39(9), 1435-1443.

Sreenivasulu, P. and N. B. Reddy (2015). Lie group analysis for boundary layer flow of Nanofluids near the Stagnation-point over a permeable stretching surface embedded in a porous medium in the presence of Radiation and Heat generation. *J. Applied Fluid Mechanics* 8(3), 549-558.

Tabanfar, S. and M. F. Modest (1987). Combined radiation and convection in absorbing, emitting, non gray gas- particulate tube flow. *J. Heat Transfer* 109, 478–484.

Yasir, K., W. Qingbiao, F. Naeem, and Y. Ahmet (2011). The effects of variable viscosity and thermal conductivity on a thin film flow over a shrinking /stretching sheet. *Computers and Mathematics with Applications* 61(11), 3391-3399.